Single diffraction and elastic scattering in proton-proton collisions with the STAR detector at RHIC*

Mariusz Przybycien

AGH University of Krakow, al. Mickiewicza 30, 30-059 Krakow, Poland

(on behalf of the STAR Collaboration)

Received November 2, 2024

The diffractive cross sections constitute a significant fraction of the total hadronic cross section in proton-proton collisions. However, due to its nonperturbative nature, the understanding of the fundamental properties of these processes highly relies on experimental studies. In these proceedings, we report the measurements of the inclusive and identified charged-hadron spectra produced via a single diffraction process in proton-proton collisions at $\sqrt{s} = 200$ GeV. In particular, we compare particle ratios of $\bar{p}/p$ and K/π to theoretical models' calculations. In addition, the first measurement of the proton-proton elastic cross section at $\sqrt{s} = 510$ GeV is presented. The dependences of the elastic cross section on the collision energy and the four-momentum transfer t are discussed and compared to model calculations for the relevant physics implications.

1. Introduction

We report on the measurements of the single diffraction (SD) process and elastic scattering in proton-proton (pp) collisions performed by the STAR [1] experiment at RHIC [2]. These two processes, characterized by the presence in the final state of one or two intact beam protons, are shown schematicaly in Fig. 1(left). STAR is especially well suited to perform diffractive-like measurements as it is equipped with the Roman Pot (RP) detection system, which allows measurements of forward-scattered beam protons at very small angles. The schematic view of the RP system is displayed in Fig. 1(right), with more detail provided in the caption. For more information on the STAR detector, see [1].

* Presented at Diffraction and Low-x 2024 meeting, 8-14 September 2024, Trabia, Sicily

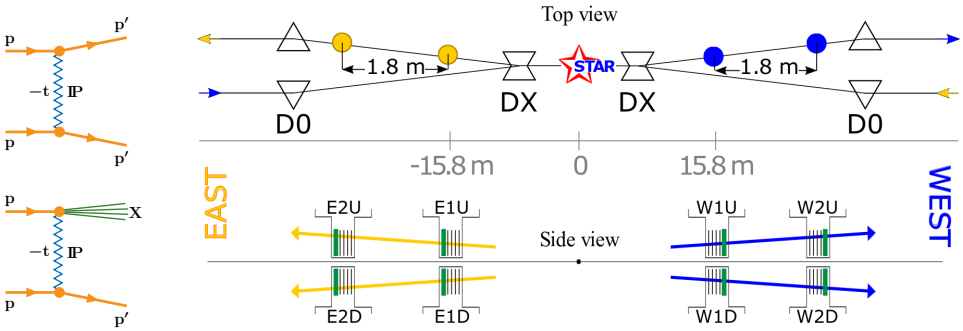

Fig. 1. (left) Diagrams for elastic scattering and single diffractive dissociation in proton-proton scattering. (right) The layout of the RP setup at STAR (not to scale) for measuring forward protons. Top (x, z) and side (y, z) views are shown. Two sets of RPs, labeled (W1, W2) and (E1, E2) were installed between the DX and D0 magnets, at 15.8 m and 17.6 m, on either side of the IP. The detector package has transverse size 5×8 cm^2 and a depth of 3.5 cm. The Si sensor is 400 μm thick, while the trigger scintillator is 5 mm thick. The strips in the Si detectors are approximately 100 μm wide. Two dipole magnets, DX and D0, which bend the beams into and out of the IP, are also shown.

2. Single diffraction production of charged hadrons

Production yields of charged-hadrons in high-energy particle collisions are among fundamental observables used to study QCD in both perturbative and non-perturbative regimes. Contribution from hard-scattering processes increases with increasing collision energy. However, soft interactions, usually modelled phenomenologically, are the most significant contribution to the number of produced particles. Measurements are necessary to constrain the free parameters of those models, and their good description is crucial for studying other QCD processes at collider experiments, especially at high luminosity regimes. Several measurements of this type exist in proton-(anti)proton, proton-nucleus and heavy-ion collisions (see, e.g. [3–5]).

Here, we present similar studies for a class of pp collisions in which one of the colliding protons escapes the collision intact at a very small angle and is measured in the RP system. In this SD process, $p+p \to p+X$, X denotes the hadronic final state produced in the interaction due to dissociation of the other beam proton. Earlier, measurements of this type were performed by the UA4 Collaboration at $\sqrt{s} = 546$ GeV in the proton-antiproton collisions at the CERN SPS collider [6].

Data used in this analysis were collected by the STAR experiment in pp collisions at $\sqrt{s} = 200$ GeV and correspond to an integrated luminosity of 15 nb^{-1}. The yields and their ratios discussed here were obtained in

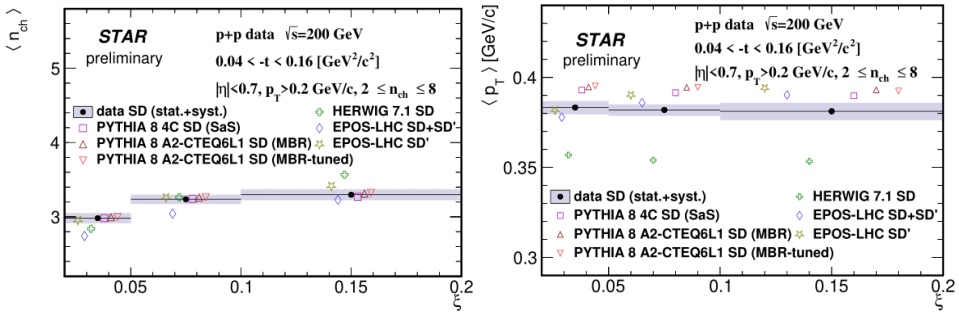

Fig. 2. (left) Mean multiplicity $\langle n_{\rm ch}\rangle$, and (right) mean transverse momentum $\langle p_{\rm T}\rangle$ of primary charged particles, shown in three ξ-intervals. Grey boxes represent statistical and systematic uncertainties added in quadrature. Predictions from MC models, shown as open symbols, are spread within bins for better visibility.

the fiducial region defined by the fractional energy loss of the diffractively scattered proton, $0.02 < \xi < 0.2$, the four-momentum transfer at the proton vertex $0.04 < -t < 0.16$ GeV$^2/c^2$ and the charged particles were required to be produced within $|\eta| < 0.7$ and have $p_{\rm T} > 0.2$ GeV. The number of charged particles produced in the final state is restricted to $2 \leq n_{\rm ch} \leq 8$.

STAR has measured multiplicity distributions of charged particles in three ξ-intervals. In Fig. 2(left) the average multiplicity $\langle n_{\rm ch}\rangle$ in each ξ-interval is shown. Data exhibit an expected increase of the $\langle n_{\rm ch}\rangle$ with ξ due to the larger diffractive masses probed at increasing ξ in the SD process. The shapes of the measured distributions are reproduced reasonably well by all PYTHIA 8 [7] models. The EPOS-LHC [8] (SD+SD′) (here SD′ denotes the EPOS events with non-diffractive flag, in which only a single proton is produced from the beam remnant) predicts much smaller $\langle n_{\rm ch}\rangle$ at $\xi < 0.1$ and HERWIG SD [9] predicts for $0.1 < \xi < 0.2$ too large value. It should be noted that EPOS-LHC SD′ describes data much better than EPOS-LHC (SD+SD′).

Densities of charged-particles have been also measured as a function of transverse momentum $p_{\rm T}$ in three ξ-intervals. In Fig. 2(right), the average transverse momentum $\langle p_{\rm T}\rangle$ in each ξ-interval is shown. Data exhibit no $\langle p_{\rm T}\rangle$ dependence on ξ. MC models describe data fairly well, predicting $\langle p_{\rm T}\rangle$ only 0.01 GeV/c higher than in data except for HERWIG SD, which predicts much steeper dependence of particle density on $p_{\rm T}$ in all three ξ ranges, which results in significantly lower predictions compared to data.

Figure 3(left) shows the ratios of production yields of $\bar{p}/p$ in three ξ-intervals as a function of $p_{\rm T}$. Data in the last two ξ ranges are consistent with equal amounts of p and $\bar{p}$ with no $p_{\rm T}$ dependence. However, in the first ξ range at $p_{\rm T} < 0.7$ GeV, data show a significant deviation from unity,

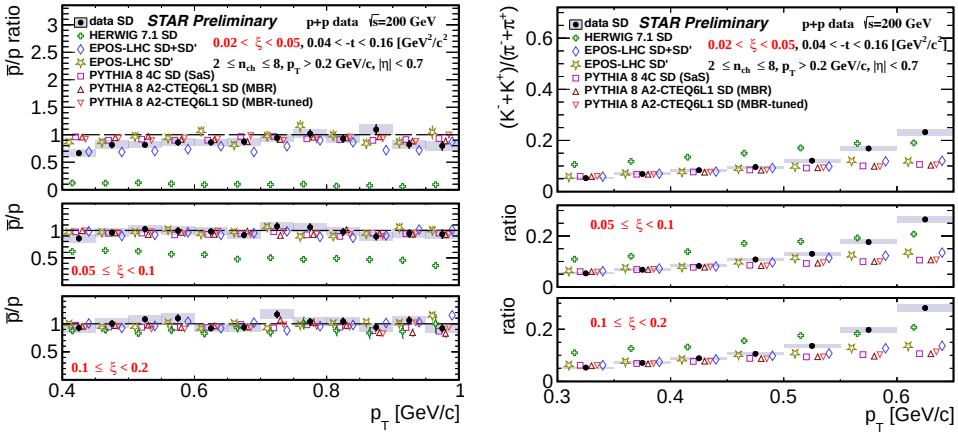

Fig. 3. Ratios of production yields of (left) $\bar{p}/p$ and (right) $(K^- + K^+)/(\pi^- + \pi^+)$, as a function of p_{T} shown in three ranges of ξ: (top) $0.02 < \xi < 0.05$, (middle) $0.05 < \xi < 0.1$, (bottom) $0.1 < \xi < 0.2$. Data are shown as full dots with error bars representing the statistical uncertainties. Grey boxes represent statistical and systematic uncertainties added in quadrature. Predictions from MC models, shown as open symbols, are spread within bins for better visibility.

indicating a large transfer of the baryon number from the forward to the central region. The data are compared to several MC models.

Figure 3(right) shows the ratios of production yields of $(K^-+K^+)/(\pi^-+\pi^+)$ in three intervals of ξ as a function of p_{T}. The ratio increases from 0.05 at $p_{\mathrm{T}} = 0.3$ GeV to 0.22−0.28 at $p_{\mathrm{T}} = 0.65$ GeV. The slope of the p_{T} dependence significantly increases at $p_{\mathrm{T}} = 0.5$ GeV in all three ξ intervals. The change of the p_{T} slope increases with ξ. All models predict similar ratios except HERWIG, which predicts values almost twice as large independently from p_{T}. PYTHIA 8 and EPOS-LHC agree very well with data at $0.3 < p_{\mathrm{T}} < 0.5$ GeV but do not expect a change of the slope of p_{T} dependence at $p_{\mathrm{T}} > 0.5$ GeV predicting rather almost twice smaller ratio at the highest p_{T}.

3. Elastic cross section measurement

Recently, STAR published a measurement of the elastic cross section in p+p collisions at $\sqrt{s} = 510$ GeV in the four-momentum transfer interval of $0.23 < -t < 0.67$ GeV^2 [10]. The data were acquired in the RHIC 2017 run during the period with special accelerator optics with $\beta^* \approx 8$ m (where β^* is the β-function value at the collision point), which resulted in a beam angular divergence of approximately 30 μrad, which is smaller than that during the standard running conditions. A similar measurement at $\sqrt{s} = 200$ GeV and

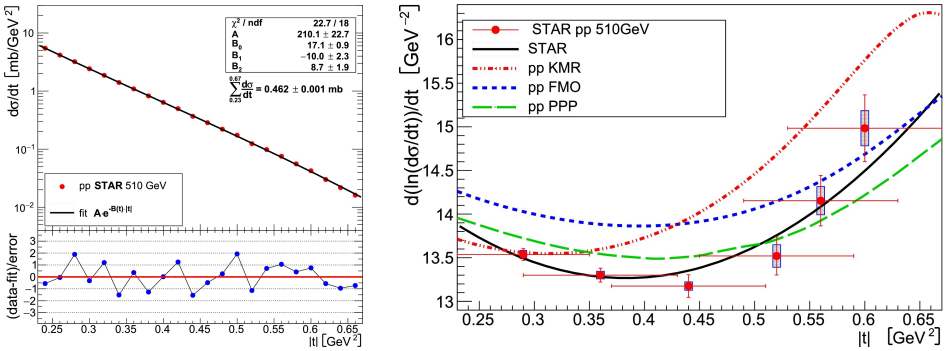

Fig. 4. (left) The pp elastic differential cross section $d\sigma/dt$ fitted with an exponential $A\exp\left[-B(t)|t|\right]$. Bottom panel: Residuals (Data - Fit)/Error. Uncertainties on the data points are smaller than the symbol size. (right) Comparison of the STAR pp results in six t sub-intervals with three models: FMO [12], KMR [13], and PPP [14]. The vertical axis is $d(\ln\left(d\sigma/dt\right))/dt$, which is a local slope B if one assumes only a constant term in the exponential. The black line is a fit to the full data set as described in the text. The horizontal size of the error bars indicates the t range where $B=$ const was fitted. The vertical size of the shaded rectangles indicates the systematic uncertainty of the data points.

smaller values of $|t|$ was published by STAR in [11].

The measured elastic cross section is shown in Fig. 3(left) together with a fit of an exponential function:

$$\frac{d\sigma_{\rm el}}{dt} = A\times\exp\left[-B(t)\cdot|t|\right] \quad \text{where} \quad B(t)=B_0+B_1\cdot|t|+B_2\cdot|t|^2$$

This non-constant assumption of B was necessary to obtain a reasonable fit. The total elastic cross section in the STAR fiducial region $0.23<|t|<0.67$ GeV^2 is $\sigma_{\rm el}^{\rm fid}=462.1\pm0.9\,({\rm stat})\pm1.1\,({\rm syst})\pm11.6\,({\rm scale})$ μb, where the scale uncertainty is related to the luminosity determination.

To characterize the shape, we fit a $B=$ const slope in six sub-intervals of t range as shown in Fig. 3(right). The vertical axis is a derivative of the logarithm of the differential cross section $d(\ln\left(d\sigma/dt\right))/dt$, which is a local slope B if one assumes only a constant term in the exponential. There is a good qualitative agreement with the three models shown. In particular, a minimum in $B(t)$ at $-t\approx0.40$ GeV^2 is observed and predicted.

4. Summary and the future perspective

The STAR experiment used its distinct possibility to tag diffractive-like events by directly measuring forward-scattered protons in the RP system to

provide new results on elastic scattering and single diffraction. The diffractive data collected by STAR will allow for new, interesting measurements.

This work was partly supported by the National Science Centre of Poland under grant UMO-2018/30/M/ST2/00395.

REFERENCES

[1] STAR Collaboration, K.H. Ackermann et al., STAR detector overview, Nucl. Instrum. Meth. A 499 (2003) 624.

[2] H. Hahn et al., The RHIC design overview, Nucl. Instrum. Meth. A 499 (2003) 245.

[3] UA1 Collaboration, G. Arnison et al., Charged particle multiplicity distributions in proton-antiproton collisions at 540 GeV centre of mass energy, Phys. Lett. B 123 (1983) 108.

[4] STAR Collaboration, J. Adams et al., Transverse-momentum and collision-energy dependence of high $p_{\rm T}$ hadron suppression in Au+Au collisions at ultrarelativistic energies, Phys. Rev. Lett. 91 (2003) 172302, arXiv:nucl-ex/0305015.

[5] ATLAS Collaboration, G. Aad et al., Charged-particle distributions in $\sqrt{s} =$ 13 TeV pp interactions measured with the ATLAS detector at the LHC, Phys. Lett. B 758 (2016) 67, arXiv:1602.01633 [hep-ex].

[6] UA4 Collaboration, M. Bozzo et al., Single diffraction dissociation at the CERN SPS collider, Phys. Lett. B 136 (1984) 217.

[7] T. Sjöstrand et al., A brief introduction to PYTHIA 8.1, Comp. Phys. Commun. 178 (2008) 852, arXiv:0710.3820 [hep-ph].

[8] T. Pierog et al., EPOS LHC: Test of collective hadronization with data measured at the CERN Large Hadron Collider, Phys. Rev. C 92 (2015) 034906, arXiv:1306.0121 [hep-ph].

[9] J. Bellm et al., Herwig 7.1 Release Note, arXiv:1705.06919 [hep-ph].

[10] STAR Collaboration, M.I. Abdulhamid et al., Results on elastic cross sections in proton–proton collisions at $\sqrt{s} = 510$ GeV with the STAR detector at RHIC, Phys. Lett. B 852 (2024) 138601, arXiv:2309.16622 [hep-ex].

[11] STAR Collaboration, J. Adam et al., Results on total and elastic cross sections in proton–proton collisions at $\sqrt{s} = 200$ GeV, Phys. Lett. B 808 (2020) 135663, arXiv:2003.12136 [hep-ex].

[12] E. Martynov, B. Nicolescu, Odderon effects in the differential cross-sections at Tevatron and LHC energies, Eur. Phys. J. C 79 (6) (2019) 461, arXiv:1808.08580 [hep-ph].

[13] V.A. Khoze, A.D. Martin, M.G. Ryskin, Elastic and diffractive scattering at the LHC, Phys. Lett. B 784 (2018) 192-198, arXiv:1806.05970 [hep-ph].

[14] V.A. Petrov, E. Predazzi, A. Prokudin, Coulomb interference in high-energy pp and anti-p p scattering, Eur. Phys. J. C 28 (2003) 525–533, arXiv:hep-ph/0206012.